Available online at www.sciencedirect.com
ScienceDirect
Inorganica Chimica Acta 359 (2006) 4901–4908
Inorganica Chimica Acta
www.elsevier.com/locate/ica

Novel organo-mineral phases obtained by intercalation of maleic anhydride–allyl ether copolymers into layered calcium aluminum hydrates

Johann Plank *, Helena Keller, Philip R. Andres, Zhimin Dai

Lehrstuhl für Bauchemie, Technische Universität München, Lichtenberstr. 4, 85747 Garching, Germany

Received 21 June 2006; received in revised form 30 August 2006; accepted 30 August 2006
Available online 5 September 2006

Dedicated to Professor Dr. Dr. h.c. mult. Wolfgang A. Herrmann.

Abstract

The work presented here deals with the intercalation of worm- and brush-shaped polycarboxylates (PC) into calcium aluminum layered double hydroxide (Ca–Al-LDH). The nanocomposite materials were obtained from tricalcium aluminate hydration in presence of polycarboxylate copolymers with different side chain lengths. As polycarboxylate compound, amphiphilic copolymers composed of maleic anhydride and α-allyl-ω-methoxy-poly(ethylene glycol) ether with side chain lengths of $n = 7$, 10, 34, 70 and 90 ethylene oxide units (EOUs) were chosen. These polymers possess a high side chain density due to strictly alternating copolymerization. Powder X-ray diffraction (XRD) of the synthesized Ca–Al–PC-LDH composites revealed that basal spacings (*d*-values) increase with the number *n* of EOUs in the side chain. An extremely high *d*-value of 4.85 nm was obtained for the polymer with $n = 34$ EOUs. According to elemental analysis data, the amounts of organic material present in the different composites were found to lie between 48 and 77 wt.%, respectively. Additionally, IR spectroscopy and thermogravimetric measurements were carried out in order to characterize the intercalates. The layered structure of the organo-mineral materials was confirmed by transmission electron microscopy (TEM).

Keywords: Layered double hydroxide; Composite materials; Polymers; Intercalation

1. Introduction

Tricalcium aluminate ($3CaO \cdot Al_2O_3$) is an important constituent and by far the most reactive phase in ordinary Portland cement [1]. Typically, 5–16 wt.% of $3CaO \cdot Al_2O_3$ occur in a cement clinker. The reactivity and hydration behavior of the aluminate phase determines the stiffening and setting behavior of the cement paste to a great extent. Therefore, it has a significant influence on the workability of cement containing products such as concrete and dry-mix mortars.

The hydration products of $3CaO \cdot Al_2O_3$ depend on the reaction temperature and the concentration of Ca^{2+} and Al^{3+} in solution. At 25 °C, tricalcium aluminate quickly hydrates to form the metastable, layered phases $4CaO \cdot Al_2O_3 \cdot 19H_2O$ and $2CaO \cdot Al_2O_3 \cdot 8H_2O$ which crystallize as hexagonal plates. Also, some solid solutions of these metastable phases with variable contents of calcium (ranging from 2.0 to 2.4) and water (ranging from 8.0 to 10.2) and amorphous, gel like $Al_2O_3 \cdot 3H_2O$ are present. The metastable phases quickly convert to the stable cubic phase $3CaO \cdot Al_2O_3 \cdot 6H_2O$ (katoite) which crystallizes cubically as rhombododecahedra. $Ca(OH)_2$ (portlandite) and γ-$Al_2O_3 \cdot 3H_2O$ (gibbsite) are formed as well [2]. $4CaO \cdot Al_2O_3 \cdot 19H_2O$ and $2CaO \cdot Al_2O_3 \cdot 8H_2O$ belong to the class of layered double hydroxides (LDHs)

* Corresponding author. Tel.: +49 89 289 13150; fax: +49 89 289 13152.
E-mail address: johann.plank@bauchemie-tum.de (J. Plank).

0020-1693/$ - see front matter © 2006 Elsevier B.V. All rights reserved.
doi:10.1016/j.ica.2006.08.038

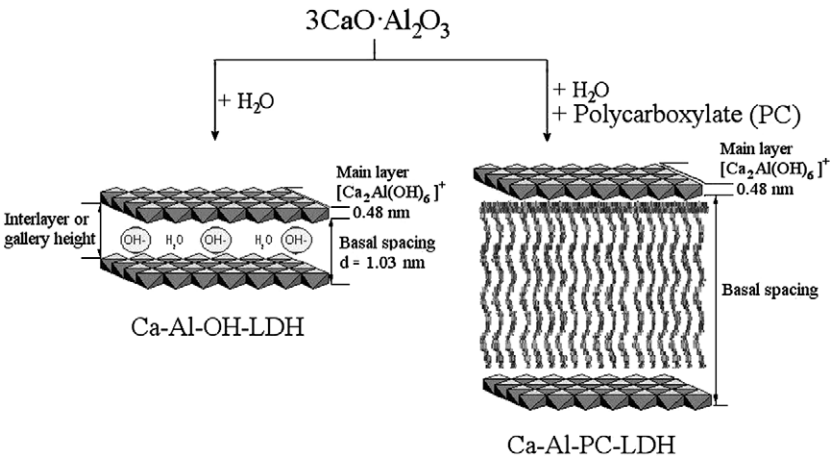

Scheme 1. Hydration products of tricalcium aluminate formed in absence and presence of polycarboxylate.

of which many examples are known [3]. Their composition is generally expressed by the formula $[M^{II}_{1-x}M^{III}_{x}(OH)_2]^{x+}\cdot X_{x/m}{}^{m-}\cdot nH_2O$ with $M^{II} = Ca^{2+}$, Mg^{2+}, Zn^{2+}, Co^{2+}, Ni^{2+}, Cu^{2+}, Mn^{2+}; $M^{III} = Al^{3+}$, Cr^{3+}, Fe^{3+}, Co^{3+}, Ni^{3+}, Mn^{3+}; X = interlayer anion, e.g., OH^-, CI^-, $NO_3{}^-$, $ClO_4{}^-$, $CO_3{}^{2-}$, $SO_4{}^{2-}$. By replacing the hydroxide ions, numerous anions can be intercalated in between the cationic main layers of LDH compounds [4]. Examples are inorganic anions such as sulfate, carbonate or nitrate and small organic molecules like oxalate, citrate or benzoate [5]. Linear polyelectrolytes such as polyacrylate, polyvinylsulfonate, polystyrene sulfonate and others are also known to intercalate between the cationic layers [6–11]. For construction applications, composites of organic perylene chromophores with Mg–Al–OH- and Zn–Al–OH-LDHs, showing brilliant colors and good photostability comparable with pigments, are also described [12].

Superplasticizers represent an important class of polyelectrolyte admixtures for use in concrete technology [13]. They are capable of enhancing the flow properties of concrete and thus reducing the water/cement ratio of concrete, resulting in higher compressive strength. Their dispersing effect derives from adsorption on the surface of hydrating cement particles, thus creating electrostatic or steric repulsion between them [14]. Many authors have pointed out that Portland cement with a high content of tricalcium aluminate interacts with high amounts of superplasticizers [15–22]. For high performance concrete where the performance of superplasticizers is a key factor, this interaction has led to the recommendation to only use Portland cement with a low content of tricalcium aluminate.

Among superplasticizers, linear β-naphthalenesulfonate formaldehyde (BNS) polycondensate has been shown not only to adsorb on the surface of tricalcium aluminate, but also to intercalate into its hydrate phase and form an organo-mineral compound, Ca–Al–BNS-LDH [23]. In a very recent study, the successful intercalation of "comb-like" polycarboxylates, another common type of superplasticizer consisting of a poly(methacrylic acid-*co*-methoxy-poly(ethylene glycol) methacrylate) with low side chain density, was accomplished [24]. The side chains grafted on to the methacrylate main chain consisted of up to 45 ethylene oxide units (EOUs). The general reaction patterns of aqueous $3CaO\cdot Al_2O_3$ in the presence and absence of such polycarboxylate superplasticizers are shown in Scheme 1.

However, up to date the intercalation of superplasticizers based on polymer brushes or star polymers with a high density of very long side chains has not been reported. Here we report on the successful intercalation of very bulky maleic anhydride–α-allyl-ω-methoxy-poly(ethylene glycol) ether copolymers into the Ca–Al-LDH structure, resulting in novel organo-mineral phases with extremely wide interlayer distances. Their formation bears importance for concrete because this type of amphiphilic copolymer is also used as superplasticizer in concrete.

2. Experimental

Tricalcium aluminate was prepared via a sol-gel process as precursor before calcination. Aqueous colloidal alumina (VP disp. W630, Degussa, Hanau, Germany) containing 29.7 wt.% Al_2O_3 with a medium particle diameter of about 200 nm was mixed with stoichiometric amounts of neutral $Ca(NO_3)_2$ solution, which was freshly prepared from $CaCO_3$ and HNO_3 (p.a. Merck, Darmstadt, Germany). The mixture was heated at 70 °C and stirred at pH 8 for 10–12 h until gel formation occurred. The gel was transferred into platinum crucibles and slowly heated to 900 °C. Water evaporated and $Ca(NO_3)_2$ decomposed to the metal oxide. Finally, the sample was heated at 1350 °C for 9 h with two intermediate grindings [25]. Investigations by X-ray powder diffraction confirmed the resulting product to be pure tricalcium aluminate.

The polymers were synthesized via radical copolymerization of maleic anhydride and α-allyl-ω-methoxy-poly(ethylene glycol) ether with $n = 7$, 10, 34, 70 and 90 EOUs [26]. The copolymers were denoted PC_n, n meaning

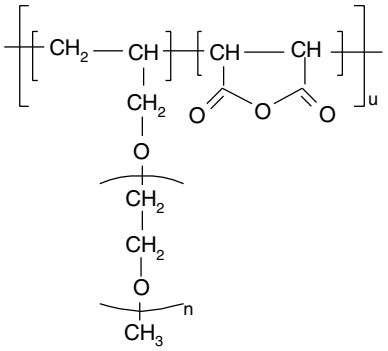

Scheme 2. Chemical structure of the synthesized allyl ether copolymers.

the number of EOUs in the side chain. Due to the fact that the monomers are not able to homo-polymerize, copolymers with a strictly alternating structure A–B–A–B are formed, thus possessing a high side chain density (Scheme 2).

From GPC measurements, the molar masses M_w and M_n as well as the hydrodynamic radii R_h were obtained (light scattering and refractive index detection). With increasing side chain length, the hydrodynamic radius R_h of the PC_n increases as expected (Table 1).

Based on the number average molecular weight (M_n), the main chain length (MCL) for each copolymer can be determined. The molar mass of a hypothetical unit comprising of 1 mol of maleic anhydride and 1 mol of allyl ether was calculated. The ratio of M_n/M_{unit} leads to the repeating number u (Scheme 2). The average backbone length of the main chain can be obtained by multiplication of the length of one unit (2×0.252 nm) with the calculated repeat number u. This calculation is based upon a C–C–C length of 0.252 nm and assumes that the polymer chain is ideally stretched. The side chain lengths (SCL) were determined in analogy to previous work by Ohta et al. [27].

According to MCL, SCL and side chain density of the synthesized polymers, the solution structure of these polymers can be classified. Gay et al. proposed a model to characterize the secondary structure of the polymers in aqueous solution [28]. According to this model, the polycarboxylates with $n = 7$, 10 and 34 EOUs have a ''worm-like'' or ''brush-like'' conformation. The macromolecule with the longest side chain ($n = 90$ EOUs) possesses a short main chain and is a star polymer. The polycarboxylate with $n = 70$ EOUs lies in between these two conformations (Scheme 3).

The Ca–Al–PC_n-LDH intercalates were prepared by the rehydration method [29]. The PC_n polymer was dissolved in 150 mL of deionized water at a concentration of 4 wt.%. Tricalcium aluminate (2 g) was added to the polymer solution (pH ~ 11.7). This suspension was stirred under argon flow at 75 °C for 70 h. Synthesis at this rather high temperature leads to larger crystals with more regularly layered stacking of the nanocomposites. Argon atmosphere was used to avoid competition between the polycarboxylate and CO_2 from air which has a high tendency to intercalate

Table 1
Characteristic properties and calculated main and side chain lengths (MCL and SCL) of the synthesized polycarboxylates

Polymer PC_n	M_w (10^3 g/mol)	M_n (10^3 g/mol)	Polydispersity index	R_h (nm)	MCL (nm)	SCL (nm)
$PC_{n=7}$	39.8	15.6	2.55	5.8	15.9	2.0
$PC_{n=10}$	53.7	19.1	2.81	6.1	15.4	2.8
$PC_{n=34}$	46.7	21.1	2.21	6.9	6.3	9.5
$PC_{n=70}$	44.9	22.5	2.00	7.5	3.5	19.6
$PC_{n=90}$	64.3	24.2	2.66	8.7	2.9	25.2

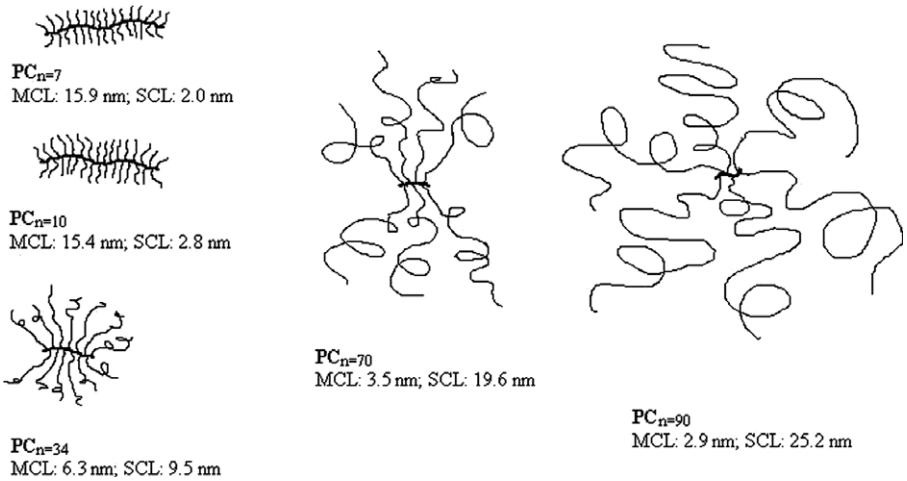

Scheme 3. Schematic representation of molecular size and conformation of the synthesized polycarboxylate copolymers.

as CO_3^{2-}. After the aging time, the precipitated composite was separated by centrifugation and washed with deionized water in order to remove residual polymer. The solid was dried for 12 h at 55 °C under high vacuum (10^{-2}–10^{-3} mbar). Under such conditions sample dryness was ensured. Ca–Al–OH-LDH was prepared by the reaction of monocalcium aluminate in deionized water [30].

Compositions of the organo-mineral compounds were determined by X-ray powder diffraction, IR spectroscopy, elemental analysis and thermogravimetry. The X-ray diffraction patterns were measured with a BRUKER axs D8 X-ray diffractometer using the Diffrac^{plus} XRD commander. The samples were ground to powder with the largest particle size being 45 μm. A silica single-crystal sample holder from BRUKER axs was used. Measurements were accomplished in continuous scan mode from the start position of 1.4° 2-Theta with a step size of 0.008384° 2-Theta (0.5 s per step). The X-ray tube (Cu Kα1,α2) was operated at a voltage of 30 kV and a current of 30 mA. For the detection, the VANTEC-1 detector from BRUKER axs was used. For the elemental analysis, C, H values were determined by conventional CHN-analysis. The Ca and Al contents were determined by analyzing dilute solutions of the synthesized PC$_n$-LDH dissolved in concentrated HNO_3 utilizing ICP-AES (SpectrAA-400). IR spectra were measured using a Fourier Transform Infrared Spectrometer FT/IR-460 Plus from JASCO Corporation. Thermogravimetric (TG) measurements were conducted with a Netzsch TG209 system. Typically, about 14 mg of sample were heated in the Al_2O_3-tube from 300 to 1473 K at 10 K min^{-1} under argon. Interpretation of the thermogravimetric data was made by using the MARSH calculation program from Netzsch. Transmission electron micrographs were recorded on a JEOL JEM 2010 microscope equipped with a LaB_6-cathode. The pictures were taken at 120 kV and at magnifications of about 100–150k.

3. Results and discussion

3.1. X-ray diffraction patterns

In spite of their bulky character and large steric size, the maleic anhydride–α-allyl-ω-methoxy-poly(ethylene glycol) ether copolymers intercalate in between the inorganic $[Ca_2Al(OH)_6]^+$-layers. The first basic reflection at low 2-Theta values corresponds to the *d*-value. It represents the basal spacing obtained from the sum of the thickness of the main layer and the distance between two layers [31,32]. A thickness of 0.48 nm for the cationic calcium aluminum hydroxide main layer has been reported earlier [33].

X-ray diffraction patterns for Ca–Al–OH-LDH and the different Ca–Al–PC$_n$-LDH intercalates are shown in Fig. 1. The first basic reflection corresponding to the highest *d*-value gives information about the interlayer distance. The diffraction pattern of inorganic Ca–Al–OH-LDH (a) reveals a strong first reflection with a basal *d*-value of 1.03 nm. High intensity with a good signal-to-noise ratio

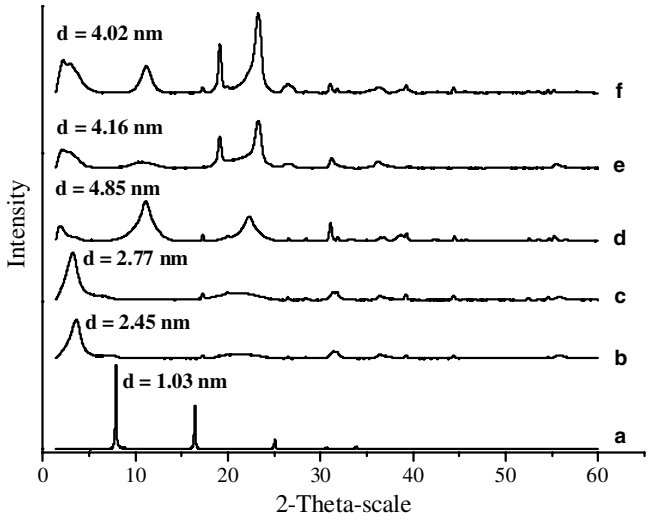

Fig. 1. X-ray diffraction pattern of Ca–Al–OH-LDH (a), Ca–Al–PC$_{n=7}$-LDH (b), Ca–Al–PC$_{n=10}$-LDH (c), Ca–Al–PC$_{n=34}$-LDH (d), Ca–Al–PC$_{n=70}$-LDH (e) and Ca–Al–PC$_{n=90}$-LDH (f) intercalates (for better comparison, the relative intensity of (a) was reduced by a factor of 20).

is typical for a substance with uniform layer stacking and orientation. The disordered layer stackings of the organo-LDHs reveal broad peaks at low 2-Theta values according to *d*-values of 2.45 nm for PC$_{n=7}$-LDH (b), 2.77 nm for PC$_{n=10}$-LDH (c), 4.85 nm for PC$_{n=34}$-LDH (d), 4.16 nm for PC$_{n=70}$-LDH (e) and 4.02 nm for PC$_{n=90}$-LDH (f). Broadness and low intensities of these peaks derive from the disordered character of the PC$_n$-LDH nanocomposites and the polydispersity of the copolymers. From the *d*-value, the gallery height can be calculated. After subtraction of 0.48 nm, the gallery heights of the Ca–Al–OH-LDH and the Ca–Al–PC$_n$-LDHs are obtained (Table 2).

Obviously, there is some dependence between the *d*-value and the corresponding side chain length of the copolymers. For the macromolecules with $n = 7$, 10 and 34 EOUs, the interlayer distance increases with increasing side chain length. Such an increase is not observed for the polycarboxylates with $n = 70$ and 90 EOUs. Comparison of the gallery heights and the SCLs indicates that for the intercalated polymer with $n = 7$, the side chains are perpendicularly orientated to the Ca–Al-LDH layer (Table 2). For the intercalated copolymers with $n = 10$ and 34, respectively, the side chains are significantly longer than the gallery heights. Consequently, the polymer side chains cannot stand perpendicular to the layer but must be tilted or compressed. The polymers with $n = 70$ and 90 EOUs produce intercalates with lower gallery heights than the copolymer with $n = 34$ EOUs. They show a shoulder peak at the first basic reflection (Fig. 1). This is not the case for the other intercalates. The reason for the appearance of an additional peak could be the intercalation of lower weight-fractions of the copolymer. However, it seems obvious that for these cases the long polymer side chains would have to lie rather flat in between the cationic layers.

Table 2
Basal spacings d and gallery heights of synthesized Ca–Al–OH-LDH and Ca–Al–PC_n-LDHs in comparison with the SCL's of the copolymers

Composite	basal spacing d (nm)	gallery height (nm)	SCL (nm)
Ca–Al–OH-LDH	1.03	0.55	
Ca–Al–$PC_{n=7}$-LDH	2.45	1.97	2.0
Ca–Al–$PC_{n=10}$-LDH	2.77	2.29	2.8
Ca–Al–$PC_{n=34}$-LDH	4.85	4.37	9.5
Ca–Al–$PC_{n=70}$-LDH	4.16	3.68	19.6
Ca–Al–$PC_{n=90}$-LDH	4.02	3.54	25.2

These results demonstrate that, similar to the more comb-like system reported earlier [24], brush- and star-shaped maleic anhydride–α-allyl-ω-methoxy-poly(ethylene glycol) ether copolymers, composed of strictly alternating monomers and therefore exhibiting a high side chain density, intercalate into Ca–Al-LDH. Remarkably, high d-values of up to 4.85 nm for the Ca–Al–$PC_{n=34}$-LDH can be observed. To our knowledge, this is the highest d-value for Ca–Al-LDH compounds reported so far.

Most remarkable is the stability of the synthesized Ca–Al–PC_n-LDHs. At room temperature and in aqueous solution, the layered structure of pure Ca–Al–OH-LDH quickly converts to the more stable cubic phase $3CaO \cdot Al_2O_3 \cdot 6H_2O$ (katoite) [1,2]. However, after the intercalation of polycarboxylates, the lamellar structure of the PC_n-LDHs is stable once it is formed. Long-term stability was proven by X-ray diffraction measurements of dried and aged composites. For example, the diffraction pattern of the synthesized Ca–Al–$PC_{n=70}$-LDH reveals no changes when remeasured after 60 days.

3.2. IR-spectroscopy

IR spectra of Ca–Al–OH-LDH and the synthesized Ca–Al–PC_n-LDH intercalates were recorded between 4000 and 400 cm^{-1}. The IR spectra of Ca–Al–OH-LDH (a) and the PC_n-LDH intercalates with $n = 10$ (b) and 90 (c) EOUs are shown as examples in Fig. 2.

The lattice vibrations of the Ca–Al-LDH structure appear at 421 cm^{-1} (Ca–O) and 530 cm^{-1} (Al–O). Around 3400 cm^{-1}, the valence vibration of water can be observed as a broad peak. The intensity of this peak depends on the content of physisorbed and crystal water of the composites. The spectra of $PC_{n=7}$-, $PC_{n=34}$- and $PC_{n=70}$-LDHs (not shown here) reveal similar bands as the spectra of

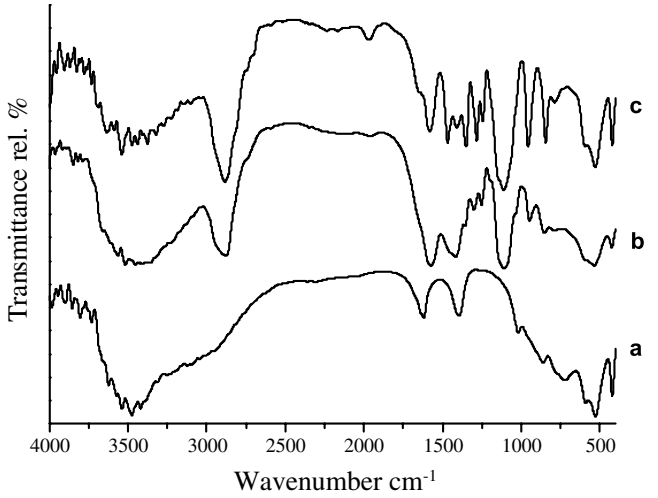

Fig. 2. IR spectra of Ca–Al–OH-LDH (a), Ca–Al–$PC_{n=10}$-LDH (b) and Ca–Al–$PC_{n=90}$-LDH (c).

$PC_{n=10}$-LDH (b) and $PC_{n=90}$-LDH (c). All spectra of the PC_n-LDH intercalates show strong bands of the C–H vibration around 2800 cm^{-1} as well as bands around 1565 and 1450 cm^{-1} which are typical for carboxylate groups. The C–O–C vibration of the ether groups of the polyethylene oxide side chains appears around 2790 and 1105 cm^{-1}. The valence vibrations of the pure copolymers are identical to those of the intercalated polycarboxylates. Consequently, the presence of the organic polymer is confirmed by the IR spectra.

3.3. Elemental analysis and thermogravimetry

In agreement with the XRD and IR results, elemental analysis of the Ca–Al–PC_n-LDH composites confirms the intercalation of the organic polymer into the layered double hydroxides. Based on the analytical data, approximate compositions for each Ca–Al–PC_n-LDH were calculated and are shown in Table 3.

For the calculation of the sum formula, the following points were considered: The molar ratio of calcium to aluminum in the nanocomposites is 2:1. The formation of $Ca(OH)_2$ and $Al(OH)_3$ is possible and has to be included. The value of the organic part can be calculated from the carbon value corresponding to one repeating polymer unit. Finally, charge compensation has to occur between the cationic inorganic layers and the anions of the interface layer (polycarboxylates and hydroxide ions).

Table 3
Chemical compositions of Ca–Al–OH-LDH and Ca–Al–PC_n-LDH intercalates

Composite	Ca (wt.%)	Al (wt.%)	C (wt.%)	H (wt.%)	organic part (wt.%)	calculated compositions
Ca–Al–OH-LDH	19.9	16.5		4.43		$Ca_2Al(OH)_7 \cdot 3.48H_2O$, $1.46Al(OH)_3$
Ca–Al–$PC_{n=7}$-LDH	14.1	4.5	28.28	6.38	52.77	$Ca_2Al(OH)_{5.72} \cdot [PC_{n=7}]_{0.64} \cdot 3.9H_2O$, $0.115Ca(OH)_2$
Ca-Al-$PC_{n=10}$-LDH	13.1	4.3	30.56	6.12	56.75	$Ca_2Al(OH)_{5.86} \cdot [PC_{n=10}]_{0.57} \cdot 3.4H_2O$, $0.056Ca(OH)_2$
Ca–Al–$PC_{n=34}$-LDH	14.5	5.2	26.04	6.04	48.27	$Ca_2Al(OH)_{6.68} \cdot [PC_{n=34}]_{0.16} \cdot 3.5H_2O$, $0.063Al(OH)_3$
Ca–Al–$PC_{n=70}$-LDH	9.0	3.2	36.01	7.12	65.83	$Ca_2Al(OH)_{6.64} \cdot [PC_{n=70}]_{0.18} \cdot 4.5H_2O$, $0.054Al(OH)_3$
Ca–Al–$PC_{n=90}$-LDH	6.3	2.2	41.71	8.03	76.68	$Ca_2Al(OH)_{6.53} \cdot [PC_{n=90}]_{0.235} \cdot 4.2H_2O$, $0.035Al(OH)_3$

The gallery heights obtained by XRD and the organic contents obtained from elemental analysis seem to be inconsistent. For example, $PC_{n=34}$-LDH possesses the greatest average gallery height, but the lowest organic content (organic part: 48.27 wt.%) of all investigated LDH composites. While the difference in the organic content is rather small when compared to $PC_{n=7}$-LDH and $PC_{n=10}$-LDH, the difference to the LDH's bearing polymers with long side chains, especially $PC_{n=90}$-LDH (organic part: 76.68 wt.%), is quite significant. A possible explanation might lie in the different intercalation conformations of the polymers which are unknown. For example, $PC_{n=90}$-LDH with its very long side chain might lie rather flat on the $[Ca_2Al(OH)_6]^+$ surface, with the polymer side chains spread out two-dimensionally, resulting in strong hydrophobic interactions between side chains of two adjacent PC molecules. This might lead to strong guest–guest interactions and a better occupancy of the interlayer space, thus giving a possible explanation for the high organic part found for $PC_{n=90}$-LDH.

Furthermore, the thermal stabilities of Ca–Al–OH-LDH and Ca–Al–PC_n-LDH composites were investigated (Fig. 3).

Two major mass losses can be observed for all synthesized composites. The first mass loss corresponds to the loss of physisorbed and interlayer water between 77 and 200 °C. Ca–Al–OH-LDH (a) lost around 4.5 wt.%. In the same temperature interval, $PC_{n=7}$- (b) and $PC_{n=10}$-LDH (c) lost around 9 wt.%, $PC_{n=34}$-LDH (d) around 11 wt.%, $PC_{n=70}$-LDH (e) and $PC_{n=90}$-LDH (f) around 5 wt.%. For the Ca–Al–PC_n-LDH composites with $n = 7$, 10, 34 and 90 EOUs, these water losses match the calculated percentages of water based on the elemental analysis reasonably well (±1 wt.%).

The second weight loss is caused by the dehydroxylation of the inorganic layers and a collapse of the layer structure [32]. Losses of 17% for Ca–Al–OH-LDH (a), 34% for $PC_{n=7}$-LDH (b), 39% for $PC_{n=10}$-LDH (c), 26% for $PC_{n=34}$-LDH (d), 54% for $PC_{n=70}$-LDH (e) and 61% for $PC_{n=90}$-LDH (f) were observed between 200 and 500 °C. Compared to the Ca–Al–OH-LDH, the higher percentage of the second weight loss in the PC_n-LDH intercalates is caused by the decomposition of the polycarboxylate molecules.

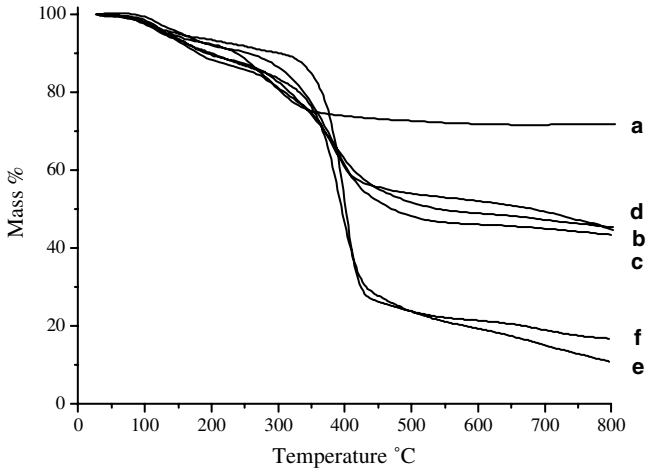

Fig. 3. Thermogravimetric data of Ca–Al–OH-LDH (a), Ca–Al–$PC_{n=7}$-LDH (b), Ca–Al–$PC_{n=10}$-LDH (c), Ca–Al–$PC_{n=34}$-LDH (d), Ca–Al–$PC_{n=70}$-LDH (e) and Ca–Al–$PC_{n=90}$-LDH (f).

3.4. TEM

The layered structure of the Ca–Al–PC_n-LDH intercalates was also confirmed by TEM. For $PC_{n=7}$-LDH (a) and $PC_{n=34}$-LDH (b) the stacking of the layers is shown in Fig. 4. The dark areas represent the skeleton of the inorganic layers, while the light areas correspond to the interlayer space harboring the organic polycarboxylates. The stacks in $PC_{n=7}$-LDH including polymer with short side chain length exist as disordered blocks within the LDH morphology. In contrast, $PC_{n=34}$-LDH (b) with a longer side chain length forms longer and more parallel orientated stacks. The formation of mostly parallel stacks was also reported from Ca–Al–PC-LDHs where the intercalated

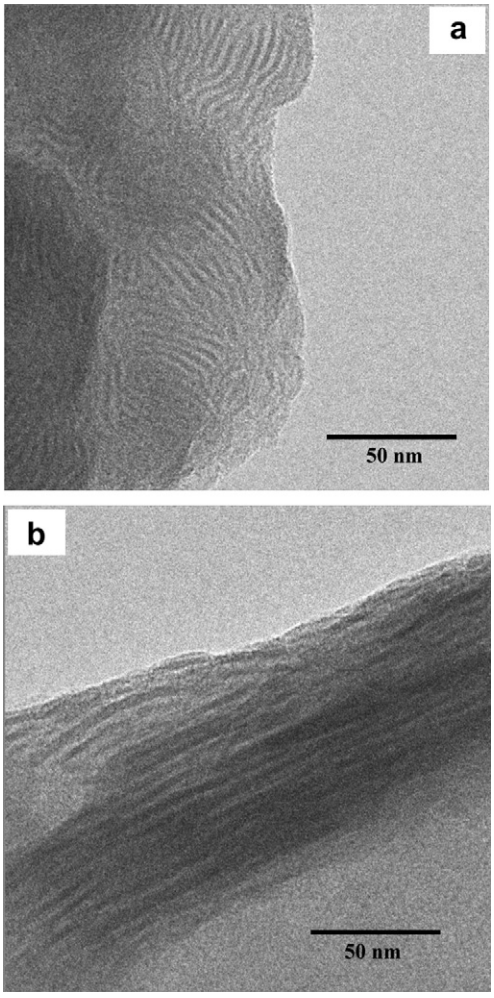

Fig. 4. TEM micrographs of $PC_{n=7}$-LDH (a) and $PC_{n=34}$-LDH (b) intercalates.

polymer was a methacrylic acid–methoxy-poly(ethylene glycol) methacrylate copolymer with low side chain density [24].

The stacking of the dark and light area has an average spacing of approx. 4 nm for $PC_{n=7}$-LDH. The light area has an average spacing of approx. 2 nm, which is in good accordance with the gallery height of 1.97 nm for $PC_{n=7}$-LDH obtained from XRD analysis. For the composites with side chain lengths of $n = 34$ EOUs and higher, only ill-defined stacking areas were observed.

4. Conclusion

We have investigated the intercalation of synthesized polymer brushes into Ca–Al-LDH obtained from tricalcium aluminate hydration by the rehydration method. Maleic anhydride–α-allyl-ω-methoxy-poly(ethylene glycol) ether copolymers bearing different side chain lengths of $n = 7$, 10, 34, 70 and 90 EOUs, showing a brush or star conformation in solution, were used as organic intercalating compound.

Surprisingly, intercalation of such sterically demanding polymer brushes is possible. XRD characterization revealed large interlayer distances caused by the polymer intercalation. A maximum gallery height of 4.37 nm was observed for the intercalate Ca–Al–$PC_{n=34}$-LDH. In spite of their high side chain density and rigid conformation, such polymer brushes exhibit a high affinity for absorption in between the cationic layers. Due to their rigidity and bulkiness, large interlayer distances are obtained. Exceptionally high contents of organic material of up to 77% were found for the composites by elemental analysis. This confirms that not only surface adsorption, but predominantly absorption (intercalation) of the copolymer has taken place. TEM images of the $PC_{n=7}$-LDH and $PC_{n=34}$-LDH intercalates confirm the existence of a layered structure. Matching values for the organic–inorganic interlayer distances can be found when comparing the TEM micrographs with the XRD results. Surprisingly, the composites have proven to be stable over a period of 2 months and do not convert to more stable cubic phases (katoite).

These results are of great importance to the field of chemical admixtures in concrete. The fact that this type of superplasticizer may intercalate into tricalcium aluminate hydrate phases indicates that this material may be lost for adsorption and not become effective as superplasticizer. From a practical point of view, it would be desirable to have a superplasticizer which only adsorbs on the surface of cement hydrate phases and does not intercalate in between the calcium aluminate hydrate layers. Such an admixture should show significant differences in the required dosages and/or the dispersing effect as well as in the final properties of hydrated cement such as compressive strength. On a more general note, such intercalates can be of importance in generating nanoporous materials through stabilization of either the organic or inorganic framework and subsequent removal of either counterpart.

Acknowledgements

The authors want to thank Nippon Oil and Fats company, Kawasaki, Japan for providing the monomers, Bernhard Sachsenhauser for the syntheses of the copolymers, Ulrike Ammari, Sabine Martinetz-Große and Thomas Tafelmaier from the micro analytical laboratory of TU Munich for carrying out the elemental analyses, and Dr. Marianne Hanzlik for taking the TEM images.

References

[1] F.W. Locher, Cement – Principles of production and use, Verlag Bau+Technik GmbH, Düsseldorf, 2006.
[2] J. d'Ans, H. Eick, ZKG International 6 (1953) 197.
[3] H.F.W. Taylor, Cement Chemistry, Academic Press, London, 1990.
[4] F. Leroux, C. Taviot-Guého, J. Mater. Chem. 15 (2005) 3628.
[5] M. Meyn, K. Beneke, G. Lagaly, Inorg. Chem. 29 (1990) 5201.
[6] S. Miyata, T. Kumura, Chem. Lett. (1973) 843.
[7] M. Tanaka, I.Y. Park, K. Kuroda, C. Kato, Bull. Chem. Soc. Jpn. 62 (1989) 3442.
[8] C.O. Oriakhi, I.V. Farr, M.M. Lerner, J. Mater. Chem. 6 (1996) 103.
[9] E.M. Moujahid, J.-P. Besse, F. Leroux, J. Mater. Chem. 12 (2002) 3324.
[10] F. Leroux, J.-P. Besse, Chem. Mater. 13 (2001) 3507.
[11] F. Leroux, P. Aranda, J.-P. Besse, E. Ruiz-Hitzky, Eur. J. Inorg. Chem. (2003) 1242.
[12] J. Bauer, P. Behrens, M. Speckbacher, H. Langhals, Adv. Funct. Mater. 13 (2003) 241.
[13] V.S. Ramachandran (Ed.), Concrete Admixtures Handbook: Properties, Science, and Technology, second ed., Noyes, Park Ridge, NJ, 1995.
[14] H. Uchikawa, S. Hanehara, D. Sawaki, Semento Konkuriito 602 (1997) 28.
[15] J. Plank, Ch. Hirsch, Seventh CANMET/ACI Conference on Superplasticizers and Other Chemical Admixtures in Concrete, ACI, SP-217 (2003) 283.
[16] E. Sakai, K. Yamada, A. Ohta, J. Adv. Concr. Techn. 1 (2003) 16.
[17] P.-C. Nkinamubanzi, B.-G. Kim, P.-C. Aitcin, Sixth CANMET/ACI International Conference on Superplasticizers and Other Chemical Admixtures in Concrete, ACI, SP-195 (2000) 33.
[18] P.-C. Aitcin, C. Jolicoeur, J.G. MacGregor, Concr. Int. (1994) 45.
[19] Ch. Hirsch, D. Vlad, J.-Y. Yang, P. Chatziagorastou, J. Plank, GDCh-Monographie Band 27 (2003) 187.
[20] K. Yamada, S. Ogawa, S. Hanehara, Sixth CANMET/ACI International Conference on Superplasticizers and Other Chemical Admixtures in Concrete, ACI, SP-195 (2000) 367.
[21] H. Uchikawa, D. Sawaki, S. Hanehara, Cem. Concr. Res. 25 (1995) 353.
[22] M.Y.A. Mollah, W.J. Adams, R. Schennach, D.L. Cocke, Adv. Cem. Res. 12 (2000) 153.
[23] V. Fernon, A. Vichot, N. Le Goanvic, P. Colombet, F. Corazza, U. Costa, Fifth CANMET/ACI Conference on Superplasticizers and Other Chemical Admixtures in Concrete, ACI, SP-173 (1997) 225.
[24] J. Plank, Z. Dai, P.R. Andres, Mater. Lett., in press.
[25] D. Stephan, P. Wilhelm, Z. Anorg. Allg. Chem. 630 (2004) 1477.
[26] J. Plank, B. Sachsenhauser, J. Adv. Concr. Techn. 4 (2006) 233.
[27] A. Ohta, T. Sugiyama, T. Uomoto, Sixth CANMET/ACI International Conference on Superplasticizers and Other Chemical Admixtures in Concrete, ACI, SP-195 (2000) 211.
[28] C. Gay, E. Raphaël, Adv. Colloid Sci. 94 (2001) 229.
[29] S. Carlino, Solid State Ionics 98 (1997) 73.

[30] P. Faucon, T. Charpentier, D. Bertrandie, A. Nonat, J. Virlet, J.C. Petit, Inorg. Chem. 37 (1998) 3726.
[31] S.P. Newman, W. Jones, New J. Chem. 22 (1998) 105.
[32] L. Raki, J.J. Beaudion, L. Mitchell, Cem. Concr. Res. 34 (2004) 1717.
[33] J.R. Smyth, D.L. Vish, Crystal Structures and Cation Sites of the Rock-forming Minerals, Allen & Unwin, London, 1988.